Supplementary Fig. 1

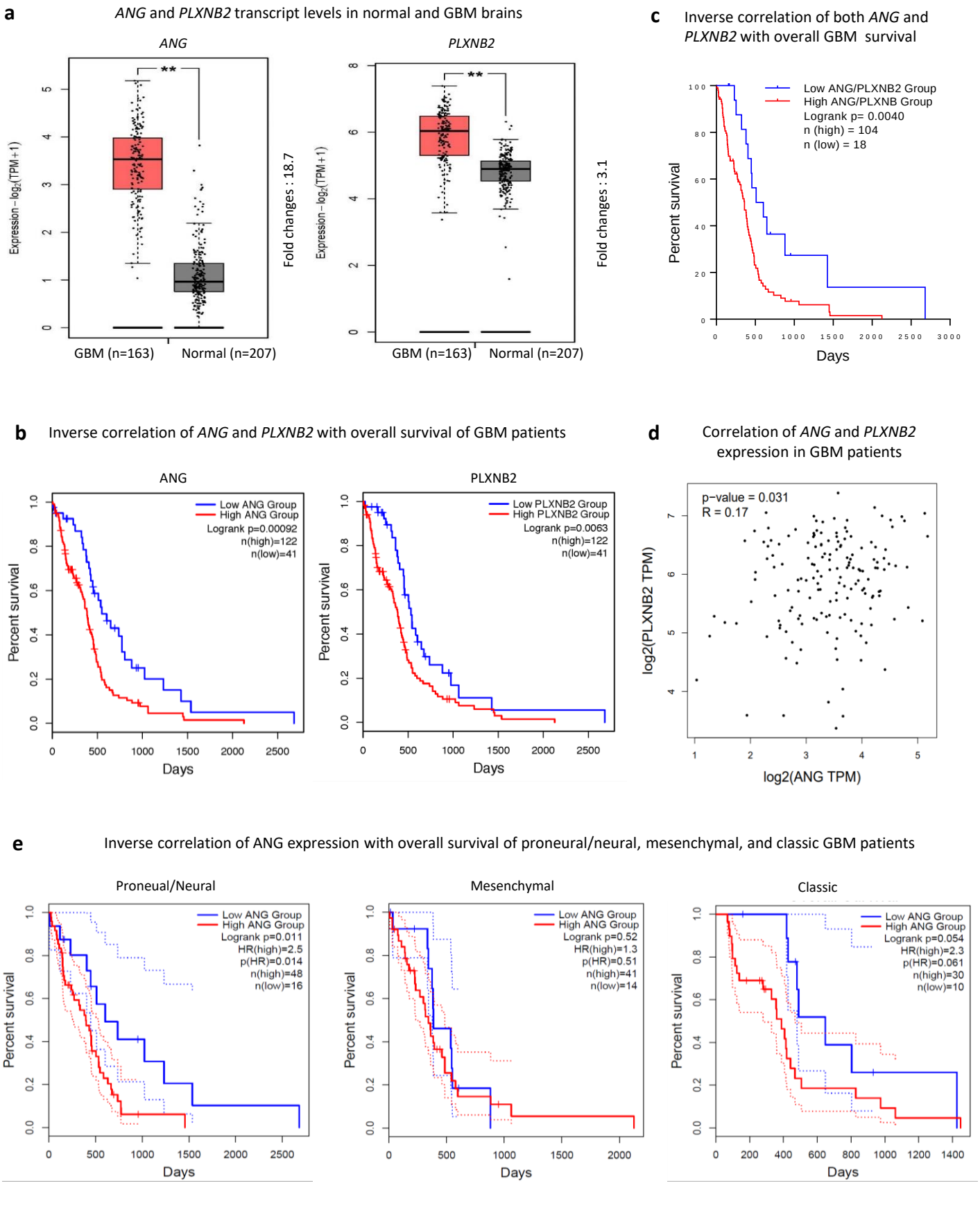

Supplementary Fig. 1. *ANG* and *PLXNB2* are up-regulated in GBM and are correlated with patient survival. a Level of *ANG* and *PLXNB2* transcripts in human GBM tissues (TCGA, Cell 2013, n = 163) and matched normal tissue (TCGA/GTEx, n = 207). Data shown is the Log_2 of transcripts per million (TPM) + 1. ** $p < 0.01$. **b** Survival plots of GBM patients (TCGA, Cell 2013, n = 163) with high (red, n = 122) and low (blue, n = 41) expression of *ANG* (left) and *PLXNB2* (right). **c** Survival of GBM patients in the same cohort with high (red, n = 104) and low (blue, n = 18) transcripts of both *ANG* and *PLXNB2*. The top 75% was defined as the high, and the bottom 25% was defined as the low in both *ANG* and *PLXNB2* expression among the 163 patients in this cohort. GEPIA2 (gene expression of profiling interactive analysis 2) program was used for transcription (**a**) and survival (**b** and **c**) analysis. **d** Correlation analysis of *ANG* and *PLXNB2* transcripts in the above cohort of GBM patients. **e** Survival plots of GBM patients of the proneural/neural, mesenchymal, and classic subtypes with high (75%) and low (25%) expression of *ANG*.

Supplementary Fig. 2

a Targeting vector for *Ang1* knockout (KO)

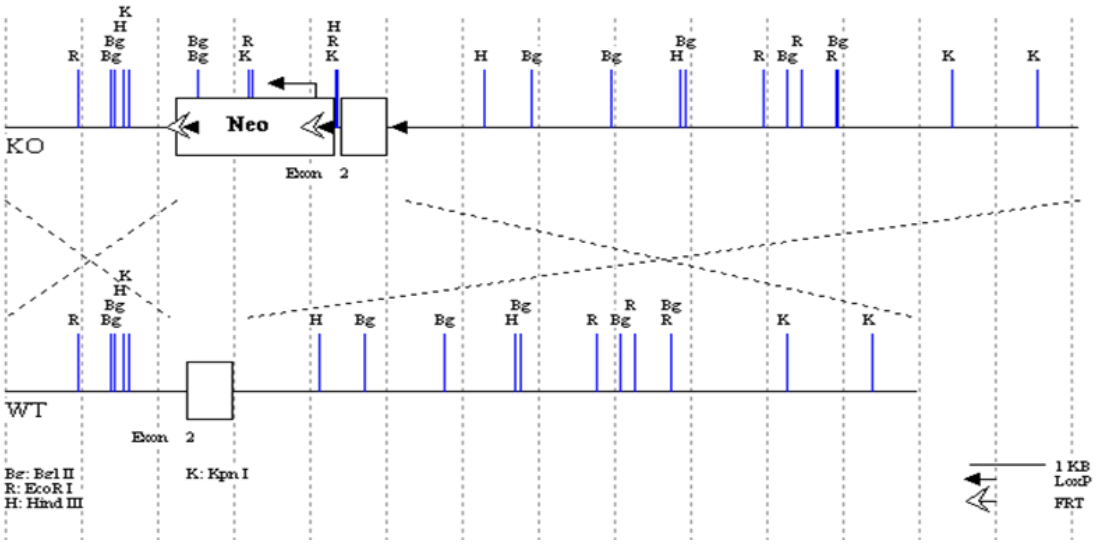

b Restriction enzyme map of targeting vector

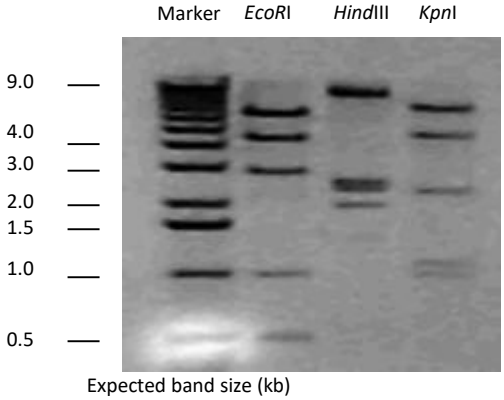

Expected band size (kb)
*EcoR*I: 0.5, 1.0,2.9, 4.5, 6.8
*Hind*III: 2.0, 2.3, 2.4, 9.4
*Kpn*I: 1.0, 1.1, 2.2, 4.5, 7.2

c PCR confirmation of ES cell clones

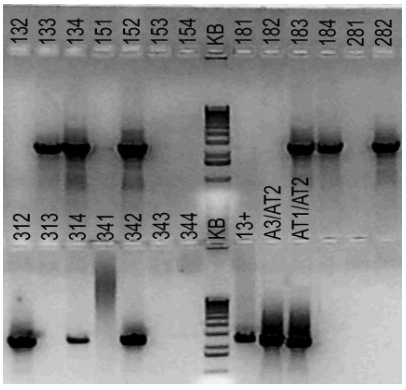

d Genotyping of F1 mice

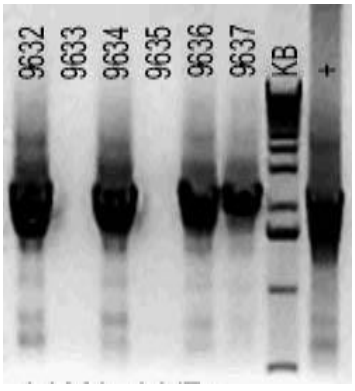

e Genotyping of *Ang1* floxed and KO mice

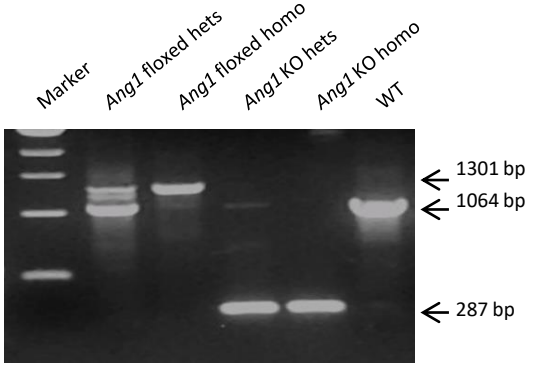

f *Ang1* mRNA and ANG protein levels

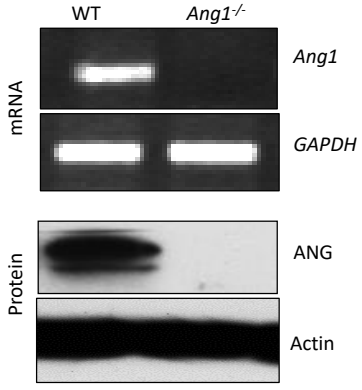

Supplementary Fig. 2. Generation of *Ang1* knockout mice. a Construction of targeting vector. A pGK-gb2 loxP/FRT-flanked Neomycin cassette was inserted 161 nt upstream from the coding exon, and an additional loxP site was inserted 80 nt downstream from the coding exon. **b** Restriction enzyme map of the targeting vector. All bands showed correct size from the targeting vector. **c** PCR confirmation of embryonic stem (ES) clones. Recombinant clones were identified by a 2.3kb PCR fragment. **d** Genotyping of F1 mice. **e** Genotyping of *Ang1* gene floxed and knockout (KO) heterozygous (hets) and homozygous (homo) mice. **f** *Ang1* mRNA and protein levels from liver tissue of *WT* and $Ang1^{-/-}$ mice.

Supplementary Fig. 3

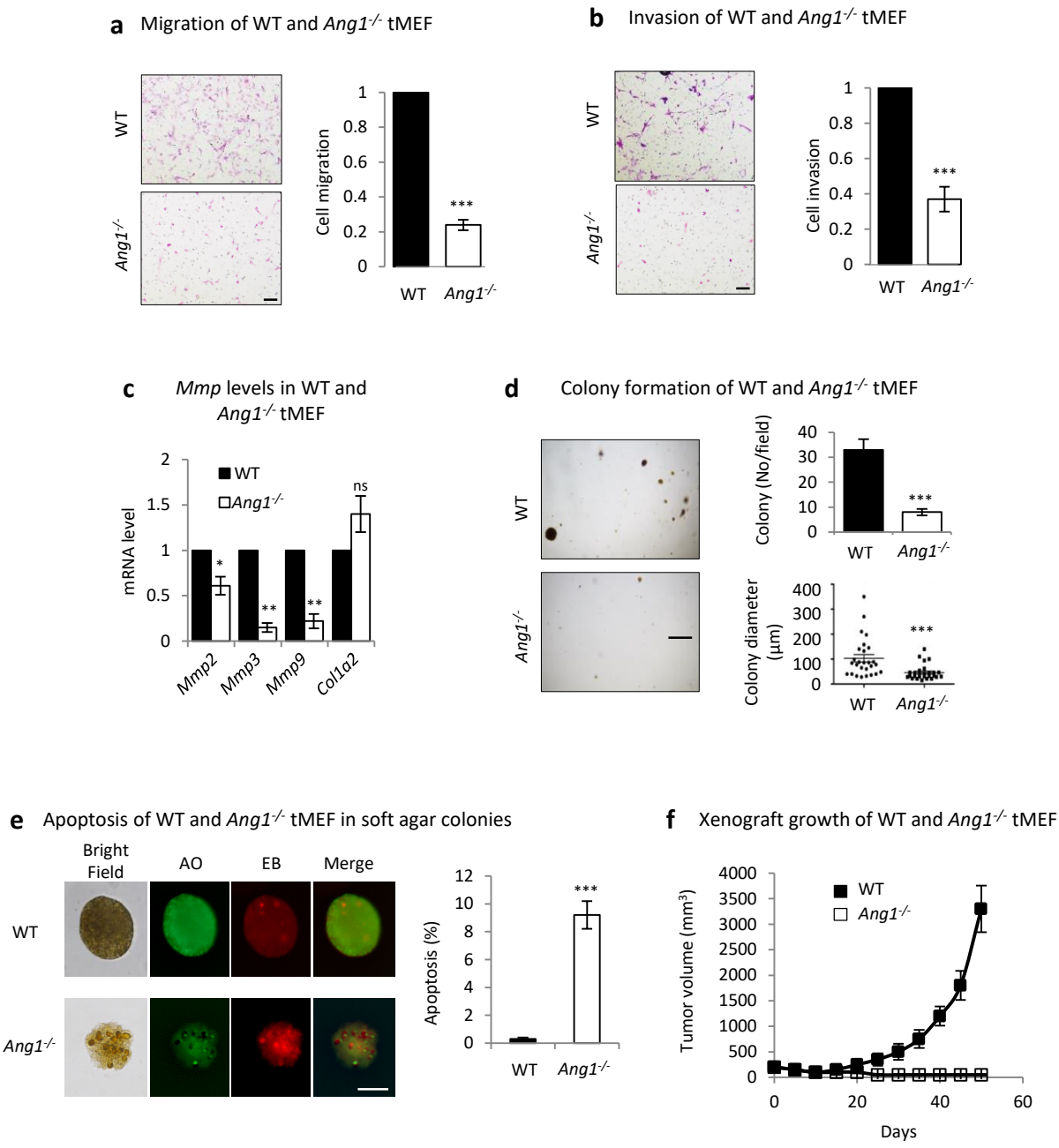

Supplementary Fig. 3. Effect of *Ang1* deficiency on transformation of mouse embryonic fibroblasts (MEF). a Trans-well migration assay. Cells migrated to the bottom of the trans-well were quantified at 24 h. Bar = 100 μm. **b** Trans-well invasion assay. The top of the insert membrane were coated with Matrigel. Bar = 100 μm. **c** qRT-PCR analysis of *Mmp2*, *Mmp3*, *Mmp9, and Col1α2* expression in WT and *Ang1*$^{-/-}$ tMEF. Data were normalized to *Gpdh* of WT tMEF. **d** Colony formation of WT and *Ang1*$^{-/-}$ tMEF. Total number of colonies per microscopic field (400 X) was counted and the diameter of each colony was measured at day 14. Bar = 500 μm. **e** AO/EB staining of representative colonies. Apoptosis was determined by the percentage of EB positive cells (red). Bar = 100 μm. **f** Ectopic growth of WT and *Ang1*$^{-/-}$ tMEF in athymic mice (n = 12). $^{**}p < 0.01$ $^{***}p < 0.001$; $^{ns}p < 0.001$.

Supplementary Fig. 4

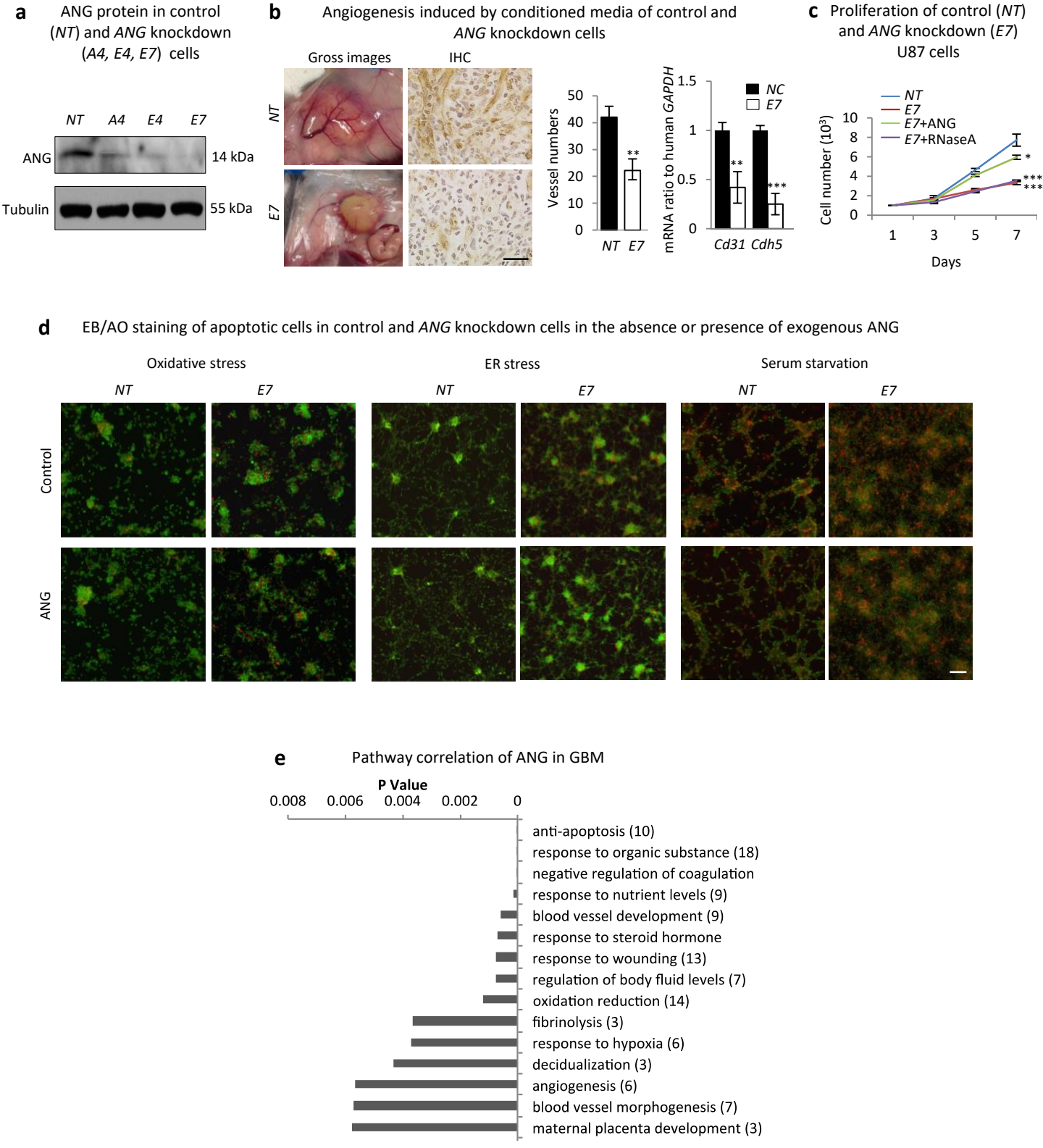

Supplementary Fig. 4. *ANG* knockdown decreased angiogenic potential of GBM cells and increased apoptosis. a Immunoblots of ANG protein in control (*NT*) and *ANG* knockdown (*A4*, *E4*, and *E7*) U87 cells. **b** Matrigel plug analysis of angiogenesis induced by control (*NT*) and *ANG* knockdown (*E7*) U87 cells. Gross images are the matrigel plugs from representative animals taken on day 6. IHC images are CD31 positive neovessels. Bar = 100 μm. Bar graphs are means ± SD of vessel numbers counted in 3 microscopic areas (400 X). The level of mouse *Cd31* and *Cdh5* (VE-Cadherin) in the matrigel was determined by qRT-PCR normalized to human *GAPDH*. **c** Proliferation of control or *ANG* knockdown U87 cells. ANG and RNaseA proteins were added at 1 μg/ml when cells were seeded. Cell numbers were determined by a Coulter counter. **d** *ANG* knockdown potentiates stress-induced apoptosis in U87 cells, which can be ameliorated by exogenous ANG protein (1 μg/ml). Apoptotic cells were stained by AO/EB in control (*NT*) and *ANG* knockdown (*E7*) U87 cells subjected to oxidative (0.25 mM sodium arsenite), ER (12.5 μg/ml tunicamycin), or serum-starvation stress for 24 h. Bar = 200 μm. **e** Pathway enrichment of genes correlated with *ANG* expression in a cohort of GBM patients (TCGA). The number of genes correlated with *ANG* in a particular pathway is shown in parenthesis. $^{**}p < 0.01$; $^{***}p < 0.001$.

Supplementary Fig. 5

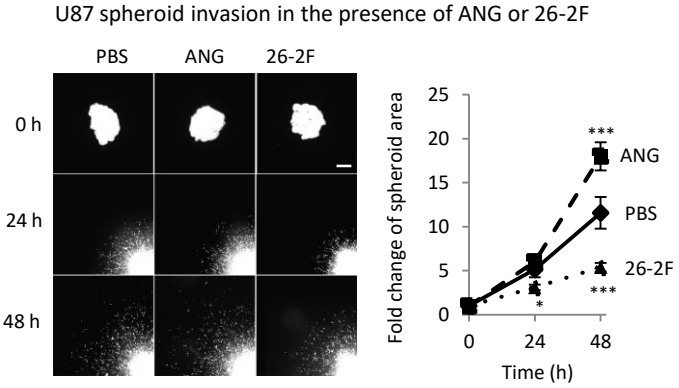

Supplementary Fig. 5. ANG mediates GBM invasion. U87 spheroid invasion in response to ANG (1 μg/ml) and anti-ANG IgG 26-2F (50 μg/ml). The invasive area was defined by the area where invaded tumor cells were found. Data shown are fold changes of spheroid area at 24 and 48 h compared to that at 0 h. Bar = 50 μm. $^{*}p < 0.05$; $^{***}p < 0.001$.

Supplementary Fig. 6

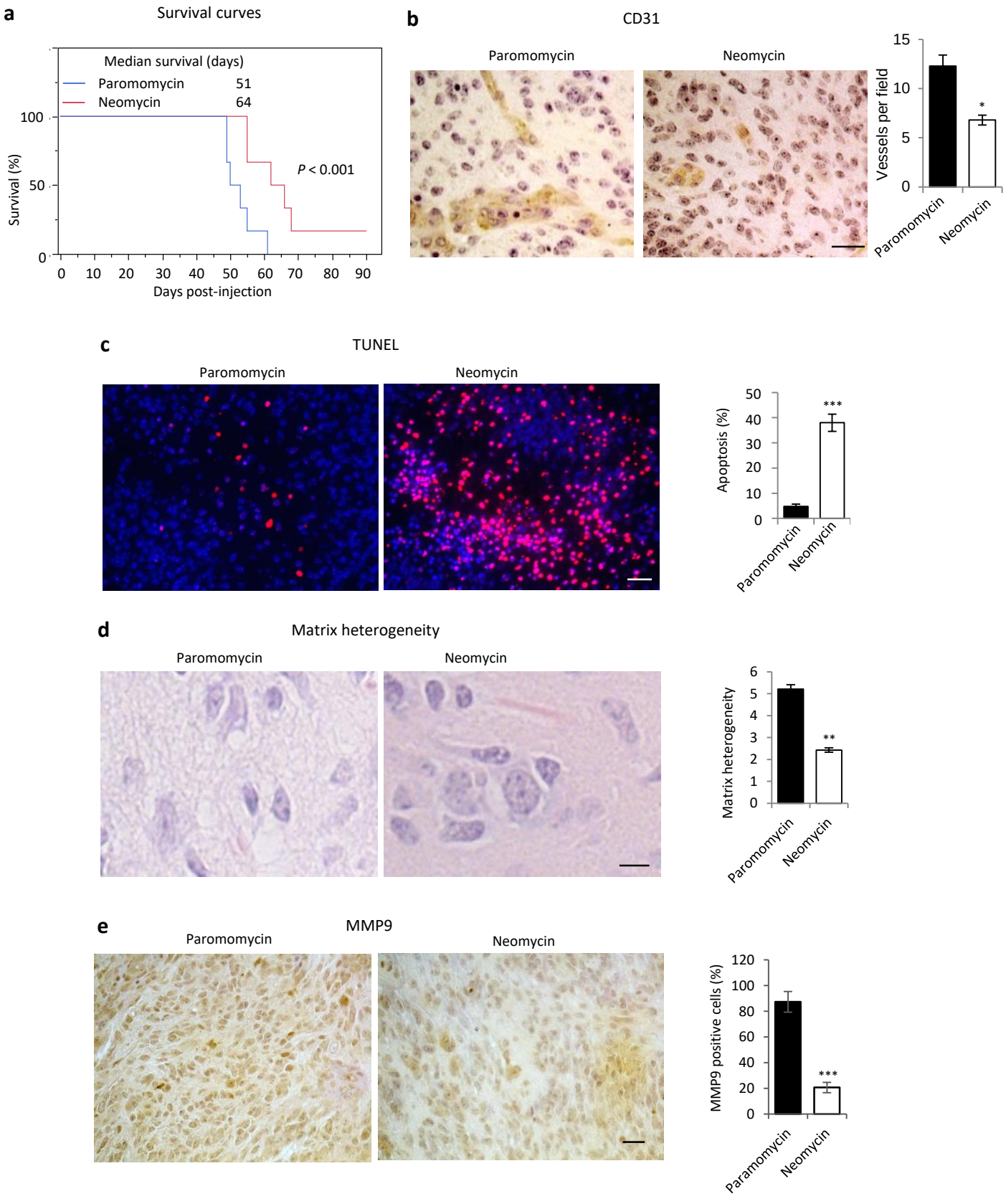

Supplementary Fig. 6. Small molecule that blocks the binding of ANG to PLXNB2 inhibits mouse GBM. a Effect of neomycin on survival of PDGF-induced GBM mice. Mouse GBM was induced as described in Fig. 1a. Two weeks after tumor induction, mice were randomly separated in two groups and treated with daily i.p. injection of 10 mg/kg of neomycin (n = 6) or paromomycin (n = 6). Numbers shown are median survival days. **b** IHC of CD31 for blood vessels. Three microscopic fields (400 X) of each sample were used for quantification. Bar = 100 μm. **c** TUNEL staining for apoptosis. The percentage of apoptotic cells was calculated from cells counted from 3 microscopic fields (400 X). Bar = 100 μm. **d** H&E staining of mouse GBM tissues. Pixels along 20 lines were measured binarily based on H&E staining and the SD of matrix reflection signal was used as indication of matrix heterogeneity. Bar = 10 μm. **e** IHC of MMP9 in drug-treated mouse GBM tissues. Bar = 100 μm. $^{**}p < 0.01$; $^{***}p < 0.001$.

Supplementary Fig. 7

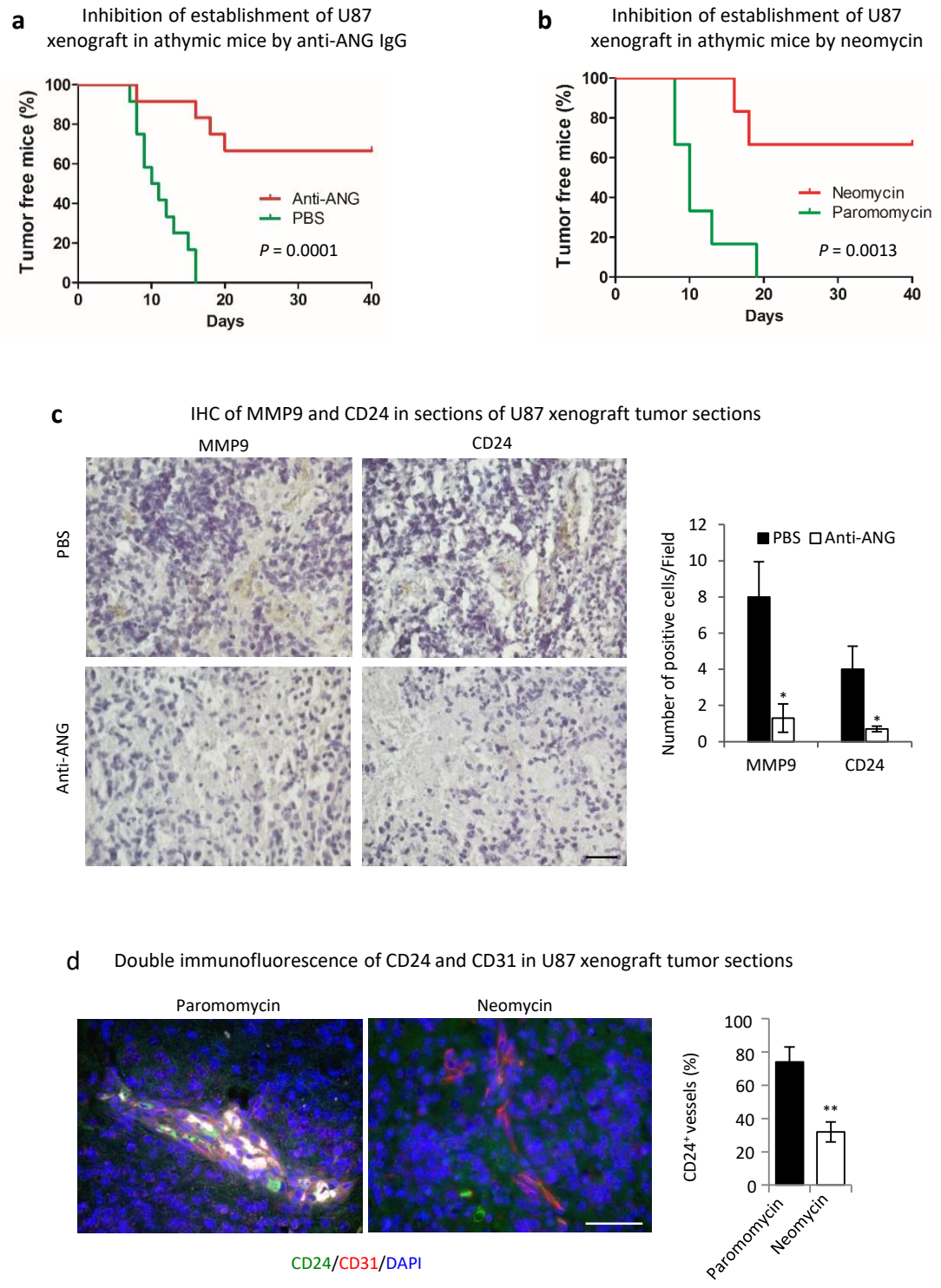

Supplementary Fig. 7. ANG inhibitors prevent the establishment of U87 xenograft tumor in athymic mice. a,b Effect of ANG mAb 26-2F (**a**) (n = 12) and small molecule inhibitor neomycin (**b)** (n = 6) on the establishment of U87 xenograft in athymic mice with PBS (n = 12) and paromomycin (n = 12) as respective controls. Treatment with daily i.p. injection of 10 mg/kg 26-2F (**a**) or 30 mg/kg neomycin (**b**) started 1 day post tumor cell (1×10^6) inoculation and continued for 28 days. **c** IHC of MMP9 and CD24 in U87 xenograft tumor sections derived from animals treated with 26-2F or PBS. Bar = 100 μm. Data shown in the bar graph are positive cells counted from 5 microscopic fields (400 X). **d** Double IF of CD24 (green) and CD31 (red) in neomycin-treated U87 xenograft tumor sections. Bar = 50 μm. Tumor cells (green) that were associated with vessels (red) were counted from 5 fields per animal (n = 3) and shown as means ± SD. $^{*}p < 0.05$; $^{**}p < 0.01$.